ChemistryEurope
Excellence in Chemistry Research Worldwide

Research Article
doi.org/10.1002/ceur.202400050

www.journal.chemistry-europe.org

Applying Metallo-Organic Ligand Design Principles to the Stereoselective Synthesis of a Peptide-Based $Pd_2L_4X_4$ Cage

Dominic F. Brightwell[+],[b] Kushal Samanta[+],[c] Jimmy Muldoon,[a] Patricia C. Fleming,[a] Yannick Ortin,[a] Lina Mardiana,[d, e, f] Paul G. Waddell,[d] Michael J. Hall,[d] Ewan R. Clark,[g] Felipe Fantuzzi,[b] and Aniello Palma*[a]

The rational and controlled synthesis of metallo-organic cages using polyaromatic ligands is well established in the literature. There is a strong interest to advance this field towards the use of chiral ligands capable of yielding cages in a stereoselective manner. Herein, we demonstrate that the classical approach for designing metallo-organic cages can be translated to polyproline peptides, a biocompatible class of chiral ligands. We have successfully designed a series of polyprolines, which mimic the topology of ditopic polyaromatic ligands, to achieve the stereoselective synthesis of a novel Pd lantern cage. This cage exhibits excellent stability in water and demonstrates the stabilization of a highly reactive species in solution. This work will pave the way towards the stereospecific synthesis of more complex, functionalized peptide-based metallo-cages.

Introduction

Inspired by nature's unparalleled control over self-assembly processes, chemists have long been pursuing the synthesis of supramolecular constructs in a controlled and predictable manner.[1,2] Metallo-organic cages are a class of discrete supramolecular non-covalent constructs for which a large set of assembly rules have been successfully established.[1–3] The seminal work of Stang, Raymond, Fujita, and Nitschke identified a number of design principles which allow the geometry of metallo-organic constructs to be predicted (e.g. cages or MOFs, M vs L ratio, geometry of the cage).[4–8] Furthermore, software developed to assist synthetic chemists to rationally design these constructs and predict their properties has recently been introduced in the literature.[9,10] However, in scoping the literature associated with these non-covalent hosts, it is evident that the large majority of ligands used are highly symmetric and are typically of a polyaromatic nature.[8,11–13] This approach is commonly used as it simplifies the assembly process (Figure 1). While some encouraging reports are appearing,[12,14,15] challenges still remain when attempting to synthesize asymmetric constructs. With the aim of developing systems closer to those found in nature, moving away from polyaromatic structures, Fujita reported the use of simple oligopeptides with pyridine units at the N and C termini. These peptides form either coordination networks or a series of complex and entangled metallo-peptide rings when exposed to metal ions (typically Ag^+).[16,17] Clever also recently reported the use of a functionalized cyclic peptide as a ligand for the synthesis of a Pd^{2+} peptide complex.[18] These reports have been instrumental in redirecting this field towards the use of biocompatible ligands. However, these impressive peptide-based nano-constructs are typically serendipitously discovered, rendering their manipulation and functionalization extremely challenging. It is evident that the design principles developed for polyaromatic ligands cannot be applied to the types of peptide-based ligands currently being reported in the literature. The classical ligands used in the assembly of metallo-cages are typically rigid (i.e., polyaromatic) and they can be treated as rod-like structures that retain their directionality throughout the self-assembly process.[8,19,20] Moreover, the bite angle,[19] the relative position of the two coordinating groups on the ligand backbone, is well defined. Therefore, structural rigidity and positional control of the coordinating groups are clearly key parameters which should be conserved in the ideal peptide-based ligand. Polyproline helices are secondary structures which appear in most proteins. In contrast to other helices used in supramolecular

[a] Dr. J. Muldoon, Dr. P. C. Fleming, Dr. Y. Ortin, Dr. A. Palma
School of Chemistry, University College Dublin, Belfield, Dublin 4, Ireland
E-mail: aniello.palma@ucd.ie

[b] Dr. D. F. Brightwell,[+] Dr. F. Fantuzzi
Supramolecular, Interfacial and Synthetic Chemistry Group, School of Chemistry and Forensic Science, University of Kent, Park Wood Rd, Ingram Building, Canterbury, CT2 7NZ, Kent, UK

[c] Dr. K. Samanta[+]
School of Chemistry, University of Birmingham, Edgbaston, Birmingham, B15 2TT, UK

[d] Dr. L. Mardiana, Dr. P. G. Waddell, Dr. M. J. Hall
Chemistry – School of Natural and Environmental Sciences, Newcastle University, Bedson Building, Newcastle upon Tyne, Tyne and Wear NE1 7RU, UK

[e] Dr. L. Mardiana
Indicatrix Crystallography Ltd, Newcastle University, Bedson Building, Newcastle upon Tyne, Tyne and Wear NE1 7RU, UK

[f] Dr. L. Mardiana
Department of Chemistry, Universitas Indonesia, Depok, Jawa Barat, 16424, Indonesia

[g] Dr. E. R. Clark
School of Science, University of Greenwich, Chatham Maritime, Chatham, ME4 4TB, Kent, UK

[+] These authors contributed equally to this work.

Supporting information for this article is available on the WWW under https://doi.org/10.1002/ceur.202400050

Research Article
doi.org/10.1002/ceur.202400050

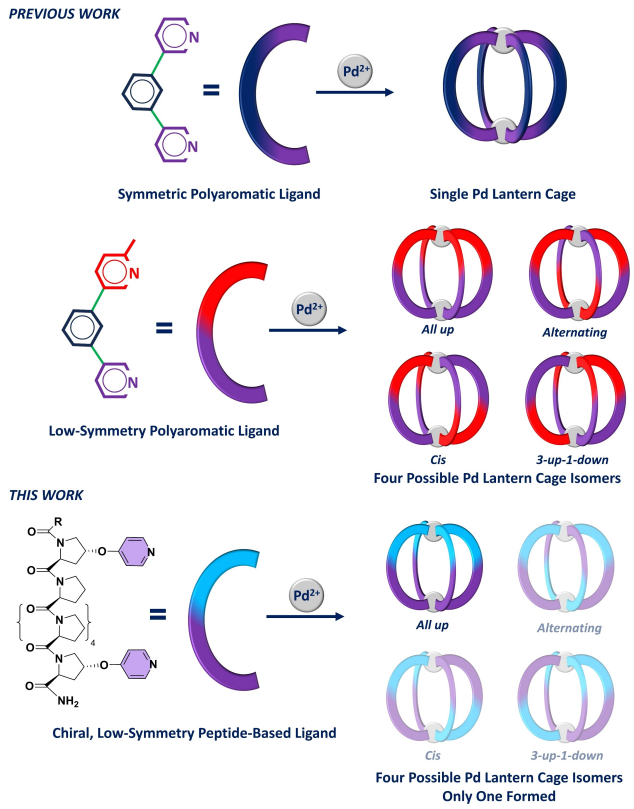

Figure 1. Schematic representation of symmetric polyaromatic ligands and low-symmetry ligands (previous work). Schematic representation of the polyproline peptide used in this work to yield a Pd lantern cage stereoselectively (this work).

chemistry, the polyproline helix is retained even in exceptionally short and un-functionalized sequences (e.g. four prolines).[21–24] We have recently demonstrated that it is possible to predict, with high accuracy, the position in space of functional groups introduced onto the backbone of polyproline helices (Figure 2a).[22] Our recent work also demonstrates the resilience of polyproline helices to functional groups, which is unparalleled when compared to other peptide-based secondary structures.[25] Therefore, the polyproline helix periodicity ($i+3$), the persistent rod-like shape,[21,26,27] and the ability to functionalize the peptide backbone with a high level of positional control,[22,28] inspired us to use these peptides as ditopic ligands in the rational synthesis of peptide-based cages. While this manuscript was in preparation, McTernan reported the use of a similar peptide system to yield palladium cages.[29] Remarkably, our system favours the formation of a different type of cage isomer. The development of these complementary methodologies offers unprecedented control in the design and synthesis of stereoselective peptide-based cages. This level of control is pivotal to the advancement of this field as we anticipate a move towards more complex and functional cages for catalysis and chemical encapsulation. These investigations were conducted simultaneously and independently by the two groups. Building upon our previous work,[21,22] herein, we successfully demonstrate that by using polyproline helices as supramolecular peptide building blocks, it is possible to translate the design principles developed for classical polyaromatic ligands to peptide-based ligands. Moreover, the peptide-based cage reported herein is able to stabilize a reactive species generated *in situ*. These findings represent an important milestone towards the future design of highly functionalized cavities capable of mimicking natural enzymes.

Results and Discussion

Design and Synthesis of the Polyproline Ligands

The first class of ligand we chose to mimic with the polyproline helix was the di-pyridine ditopic ligand typically employed with Pd^{2+} salts to synthesize lantern shaped metallo-cages.[7] We have recently demonstrated via SC-XRD, that the hydroxyl groups of *trans*-hydroxyproline (Hyp) in the peptide AcHyp-Pro-Pro-HypNH$_2$ are facing away from the peptide backbone and on the same polyproline face (Figure 2a).[22] This spatial arrangement mimics the classical C shape of ditopic ligands used in the synthesis of lantern shaped Pd^{2+} cages. We hypothesized that further functionalization with a coordinating group would result in a peptide-based ditopic ligand which should follow the same predictable behavior as the classical polyaromatic ditopic ligands. Two non-natural proline based amino acids were synthesised. The introduction of the coordinating group on position 4 of the proline was achieved starting from protected *cis*-hydroxyproline, proceeding via a Mitsunobu reaction using

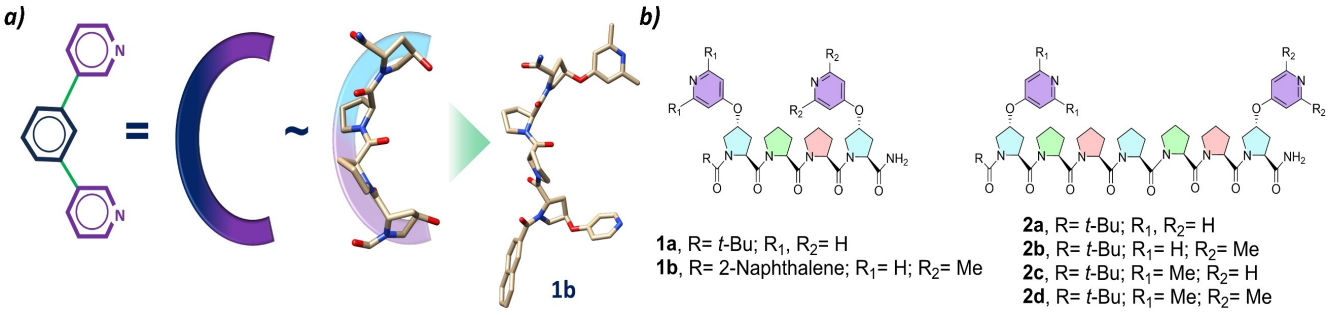

Figure 2. a) Schematic representation of a classical ditopic aromatic ligand and SC-XRD of AcHyp-Pro-Pro-HypNH$_2$ and **1b**, used to demonstrate how their spatial arrangement mimics the classical C shape of ditopic aromatic ligands. b) Polyprolines used in this work. Proline rings color-coded according to their helical face.

Research Article
doi.org/10.1002/ceur.202400050

either 4-hydroxypyridine and 2,6-dimethyl-4-hydroxypyridine as a nucleophile (ESI section 2). Full deprotections, followed by Fmoc protection of the amine, yielded the desired non-natural Fmoc protected prolines in good yields. Using Fmoc based methodology on solid phase peptide synthesis (SPPS), polyprolines **1a**–**b** and **2a**–**d** were synthesized and purified by preparative HPLC (Figure 2b, ESI section 2). The formic acid salts of the peptides **1a**–**b** and **2a**–**d**, obtained upon HPLC purification, were converted into the deprotonated free form using ion-exchange resin (ESI section 2). Using the synthetic methodology described above, we were able to introduce the coordinating groups (i.e. pyridine and lutidine) near the polyproline chiral helical backbones. We anticipated that their proximity would have a positive impact on the stereoselective synthesis of our peptide-based Pd cages. To our delight, we were able to crystallize compound **1b** from slow evaporation of a saturated methanol solution, to provide single crystals suitable for single crystal X-ray diffraction analysis. Compound **1b** crystallized in the orthorhombic space group $P2_12_12_1$, with large solvent-accessible voids along the crystallographic [100] direction. The contents of these voids are assumed to be methanol, disordered over multiple positions, but a suitable model was not forthcoming and the associated electron density was hence treated using the Olex2 solvent mask routine (ESI section 5). We were pleased to observe that despite the high level of functionalization of **1b**, in line with our previous work, the SC-XRD analysis of the structure confirmed that both the predicted absolute stereochemistry (Flack parameter = 0.07(14)) and the polyproline II secondary structure had been retained (Figure 2a).[21,22] Peptide **1a** was capped with a pivalic amide at the N-terminus to remove any rotamers in solution as observed for **1b** (ESI figure S54), hence simplifying the interpretation of the NMR data.[30]

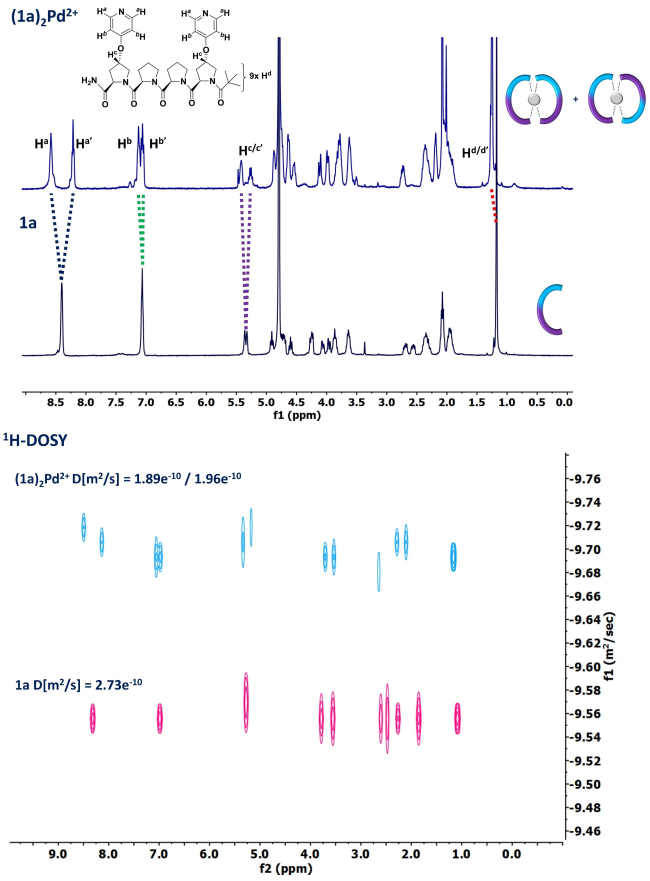

Figure 3. Stacking of ^{1}H-NMR and ^{1}H-DOSY for **1a** and **(1a)$_2$Pd^{2+}**. DOSY f1 scale is logarithmic; Hydrodynamic radius calculated for **(1a)$_2$Pd^{2+}** of ~11 Å and ~10 Å, which is in good agreement with molecular modelling, see table S3 in the ESI.

Pd^{2+} Complexation by the Polyproline Ligands

All peptides were soluble in water and D_2O. A solution of **1a** in D_2O was treated with 0.5 eq of $Pd(MeCN)_4(BF_4)_2$ and heated at 338 K for 2 h. ^{1}H-NMR and ^{1}H-DOSY analysis showed full conversion of **1a** into a mixture of two species (Figure 3; D[m^2/s] = 1.89 e^{-10} and 1.96 e^{-10}). LC-HRMS showed that the species present in solution were doubly charged. The chromatogram trace showed two peaks each with the same mass, charge, and isotopic patterns (ESI figure S62). These results suggest that the polyproline tetramer **1a** behaves like a chelating ligand forming a ML_2^{2+} complex, rather than the desired $M_2L_4^{4+}$ cage. We concluded that the two species in solution were the two isomers of **(1a)$_2$Pd^{2+}** (DFT models of these two complexes can be found in the ESI figure S80). As polyproline helices show a periodicity of $i+3$, the heptameric peptide **2a** was synthesized with the intention of preparing an elongated ligand with the same topology as **1a**–**b**. We hypothesized that the spacing between the two pyridine groups in **2a** would promote the formation of the desired **(2a)$_4$Pd$_2^{4+}$** cage. A solution of **2a** was treated with 0.5 eq of $Pd(MeCN)_4(BF_4)_2$ and heated at 338 K for 2 h. ^{1}H-NMR analysis showed conversion of **2a** into a single new species and HRMS confirmed this species to be the desired tetra charged lantern cage (Figure 4). 1D, 2D and ^{1}H-DOSY NMR analysis confirmed the presence of a single species in solution. Circular dichroism (CD) studies showed that **2a** and **(2a)$_4$Pd$_2^{4+}$** retained the polyproline II conformation (ESI figure S77). In the case of asymmetric ligands such as **2a**, there are four possible $Pd_2L_4^{4+}$ isomers that can form in solution (see figure 1); remarkably, **(2a)$_4$Pd$_2^{4+}$** is formed in a stereoselective manner. Of the four possible cage isomers, due to their symmetry, only two of them can yield a ^{1}H-NMR spectrum which is consistent with the one obtained for **(2a)$_4$Pd$_2^{4+}$**, the *all-up* or the *alternating* isomer. The *3-up-1-down* isomer can be excluded as this would yield a highly complex ^{1}H-NMR, as each peptide pillar would be in a different chemical environment. The *cis* isomer can also be excluded as its symmetry would yield a ^{1}H-NMR spectrum with double the number of signals compared to **2a** (e.g. the tert-butyl would show as two singlets, each integrating for eighteen protons). As both sets of aromatic peaks for the pyridines at the N and C terminals overlap in the complex and in **2a** (Figure 4), NOESY NMR could not be used to interrogate the geometry of this isomer (ESI figure S46). Moreover, attempts to crystallize this cage were unsuccessful. To probe the geometry of **(2a)$_4$Pd$_2^{4+}$** around the metal centres, we decided to modulate the steric bulk of the pyridyl groups.

Research Article
doi.org/10.1002/ceur.202400050

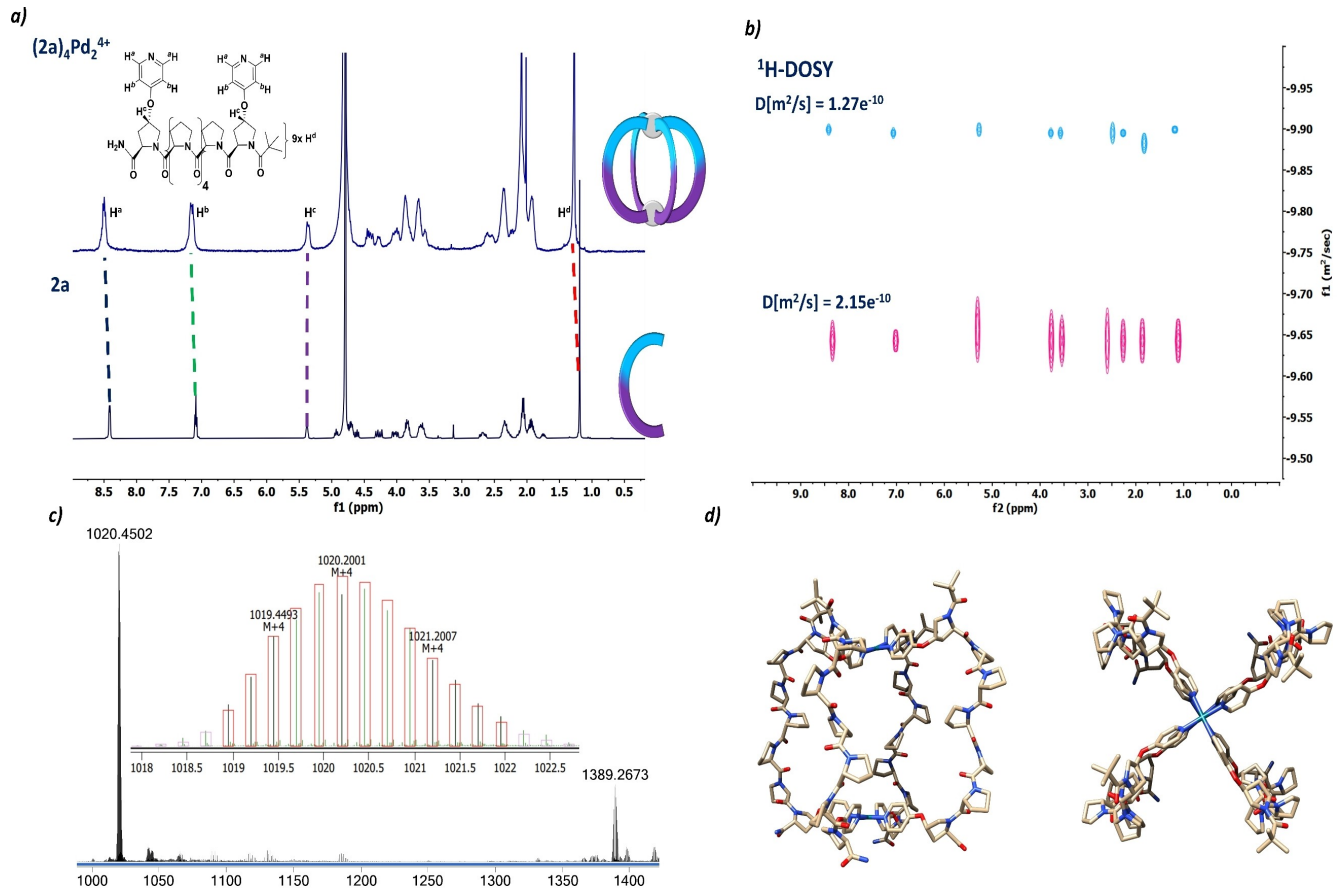

Figure 4. a) Stacking of ^{1}H-NMR and b) ^{1}H-DOSY for **2a** and **(2a)$_4$Pd$_2^{4+}$**. DOSY f1 scale is logarithmic; Hydrodynamic radius calculated for **(2a)$_4$Pd$_2^{4+}$** of ~15 Å which is in good agreement with molecular modelling, see table S3 in the ESI; c) HRMS spectra and HRMS isotopic pattern for the tetra charged complex. The red boxes encompassing the measured peaks denote the calculated isotopic pattern for the tetra charged complex with bounds set to calculated isotopic abundances and a permitted mass deviation of +/- 5 ppm; d) Side view and top view of **(2a)$_4$Pd$_2^{4+}$** model (ESI section 8 for details), hydrogens are removed for clarity.

We hypothesised that if the peptides in **(2a)$_4$Pd$_2^{4+}$** are in the *all up* conformation, the assembly of peptides **2b–c** into cages would not be successful as the steric demand around the Pd centre coordinating the four lutidines would be too high.

On the other hand, if it is the alternating isomer which is forming in solution, treatment of **2b–c** with Pd^{2+} salt should yield a lantern cage as the major product, as the steric demand would be much lower in this case, with two lutidines coordinating to each metal centre.[31] In support of our hypothesis, peptide **2d** successfully demonstrated that the lantern geometry could not be achieved with four lutidines around the metal centre, as no complex formation occurred when **2d** was treated with 0.5 eq. of $Pd(MeCN)_4(BF_4)_2$ (see NMR analysis in ESI figures S56, S59 and S60). When **2b** and **2c** are treated separately with Pd^{2+} salt, complicated mixtures of products were observed in the ^{1}H-NMR with some organic precipitate forming in both cases (ESI figures S54–S55). These results suggest that cage **(2a)$_4$Pd$_2^{4+}$** adopts the *all-up* geometry. To explore this further, a detailed computational investigation of the four possible isomers was performed based on distinct computational approaches. Given the large size of the systems, each containing nearly 550 atoms, full density functional theory (DFT) calculations for obtaining optimized geometries were impractical. Therefore, we performed geometry optimizations using four distinct approaches : (1) modeling the full systems with the semi-empirical PM6 method;[32] (2) describing the full systems with Grimme's extended semi-empirical tight-binding GFN2-xTB method;[33] (3) the ONIOM approach combining DFT calculations for both the Pd atoms and the surrounding pyridine ligands, with GFN2-xTB for the other atoms; and (4) classical molecular mechanics (MM) with the universal force field (UFF)[33] coupled with SAMSON's automatic molecular structure perception.[34] Detailed descriptions of these approaches are provided in the supplementary information. Of these approaches, the optimization of the cages through classical molecular mechanics (MM) with the universal force field (UFF)[33] coupled with SAMSON's automatic molecular structure perception was successful and smoothly led to reasonable cage structures.[34] Single-point calculations at the PBE0[35,36]-D3[37](BJ)[38]/def2-SVP[39] + SMD[40](water) level of theory on the optimized cages, after DFT re-optimization of the hydrogens, revealed a slight preference for the *all-up* geometry over the other three isomers, with the *all-up* geometry being more stable than the *alternating* structure by 1.93 kJ mol^{-1}. The

Research Article
doi.org/10.1002/ceur.202400050

calculated energies associated with each possible isomer follow a clear trend; a gradual increase in energy directly proportional to the number of antiparallel helices in the cage (ESI table S1). These calculations align well with our experimental observations.

$(2a)_4Pd_2^{4+}$ Stability and its Interaction with a Reactive Species

The stability of the $(2a)_4Pd_2^{4+}$ was monitored via NMR studies. ^{1}H- and ^{19}F-NMR spectra were recorded for the same sample stored at room temperature in an NMR tube over a period of four months (Figure 5 a). While no decomposition of the cage was observed in the ^{1}H-NMR (ESI figure S49), after a few months a new peak emerged in the ^{19}F-NMR spectrum (Figure S50b). The chemical shift of this peak (−131.47 ppm, internal reference TFA) and the presence of satellite peaks consistent with a ^{29}Si-^{19}F coupling (108 Hz), indicate that this species is $[SiF_6]^{2-}$.[41] A ^{29}Si-^{19}F HSQC experiment confirmed the presence of a silicon atom (−188.32 ppm) directly bound to the fluorine atoms at −131.47 ppm (Figure 5b). The silicon chemical shift is consistent with literature reports for $[SiF_6]^{2-}$. The formation of $[SiF_6]^{2-}$ *in situ* is due to the slow decomposition of BF_4^- in aqueous environment[42] (pH 7.4) in a silicate glass tube. However, we were surprised to record the absence of the F^- ions in solution (expected peak at ~ −127 ppm), which would be expected to appear from the slow decomposition of free $[SiF_6]^{2-}$ in unbuffered D_2O.[43,44]

Metallo-organic cages capable of stabilizing a reactive species have been reported in the literature,[45–47] and our data suggests that $(2a)_4Pd_2^{4+}$ behaves in a similar manner. We hypothesize that $(2a)_4Pd_2^{4+}$ is engaging with the reactive anion $[SiF_6]^{2-}$, preventing its hydrolysis. ^{1}H–^{19}F HOESY experiments were performed to probe our hypothesis and investigate any supramolecular engagement of the anion with the peptide cage. Through space correlation between the fluorine signal at −131.47 ppm and the aromatic proton of the pyridine at 8.52 ppm of $(2a)_4Pd_2^{4+}$ was established by ^{1}H–^{19}F HOESY experiments (Figure 5c; ESI figure S52). As a control experiment, we checked the stability of a sample of $(1a)_2Pd^{2+}$ left in D_2O at room temperature for several months (ESI figure S42a–c). Interestingly, in contrast to what we observed for the cage solution, ^{1}H-NMR analysis showed decomposition of the $(1a)_2Pd^{2+}$ complexes (ESI figure S42a). The ^{19}F-NMR spectrum showed the presence of $[SiF_6]^{2-}$ (−130.48 ppm, confirmed by ^{29}Si–^{19}F HSQC figures S42b–c) and F^- ions in solution (−127.28 ppm, ESI figure S42b). The reactivity of $[SiF_6]^{2-}$ generated *in situ* in the $(1a)_2Pd^{2+}$ sample was clearly different from that observed in the peptide cage solution. These results suggest that the enhanced stability of $[SiF_6]^{2-}$ in the peptide cage solution is due to the formation of a host-guest complex between $[SiF_6]^{2-}$ and the $(2a)_4Pd_2^{4+}$ cage; a type of supramolecular complex which cannot form with $(1a)_2Pd^{2+}$ as it lacks a cavity. This hypothesis is further supported by the downfield shift in the ^{19}F NMR spectrum for the $[SiF_6]^{2-}$ generated *in situ* in the $(1a)_2Pd^{2+}$ solution (ESI figure S53).

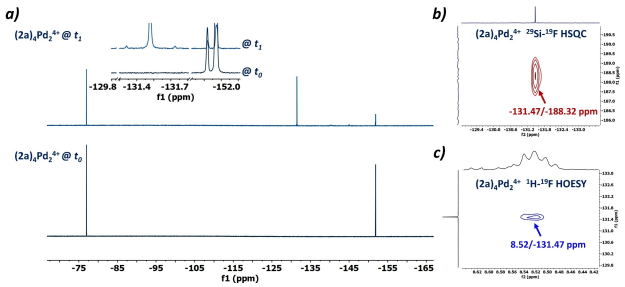

Figure 5. a) Stacking of ^{19}F-NMR spectra at t_0 (recorded as soon as synthesized) and t_1 recorded after four months. b) ^{29}Si-^{19}F HSQC and c) ^{1}H–^{19}F HOESY spectra of $(2a)_4Pd_2^{4+}$ demonstrating through space engagement between the cage and $[SiF_6]^{2-}$.

Conclusions

In conclusion, we have successfully demonstrated the controlled, stereoselective synthesis of a novel polyproline-based Pd-cage. We have demonstrated that the classical approach towards the rational design of metallo-organic cages can be translated to polyproline helices. This class of peptides offers the rigidity and positional control of functional groups, typically associated with classical polyaromatic building blocks, but with the added advantage of being chiral. The peptide cage reported herein shows remarkable stability in aqueous solution. Furthermore, we have demonstrated its ability to engage in host-guest complexation which has led to enhanced stability of the silicon hexafluoride ion formed *in situ*. Future work will explore the ability of these polyproline-based cages to act as catalysts capable of stabilizing charged and reactive intermediates. These findings will pave the way towards the stereospecific synthesis of more complex, functionalized peptide cages for applications in host-guest chemistry, catalysis, and chemical separation. These results will be reported in due course.

Acknowledgements

AP, DFB and KS thank EPSRC (grant EP/T016140/1) for their generous financial support. FF acknowledges the financial and computational support provided by the University of Kent and Julius-Maximilians-Universität Würzburg. Special thanks are extended to Dr. Timothy Kinnear for his invaluable assistance with high-performance computing. JM thanks the Comprehensive Molecular Analysis Platform (CMAP) initiative under the SFI Research Infrastructure Programme in 2019 (grant 18/RI/5702) for the generous support of the LCMS facilities. PCF, YO thank SFI (grant 12/RI/2341) and UCD Equip Funding Programme – 2020 and 2022 for the generous support of the NMR facilities. MJH, LM and PGW thank the Engineering and Physical Sciences Research Council (grant EP/W021129/1) for single crystal X-ray diffraction facilities.

Research Article
doi.org/10.1002/ceur.202400050

Conflict of Interests

The authors declare no conflict of interest.

Data Availability Statement

The data that support the findings of this study are available from the corresponding author upon reasonable request.

Keywords: peptide-based metallo-cages · supramolecular chemistry · polyproline · peptide-based supramolecular chemistry · host-guest systems

[1] M. Raynal, P. Ballester, A. Vidal-Ferran, P. W. N. M. Van Leeuwen, *Chem. Soc. Rev.* **2014**, *43*, 1734–1787.
[2] S. Pullen, J. Tessarolo, G. H. Clever, *Chem. Sci.* **2021**, *12*, 7269–7293.
[3] C. J. Brown, F. D. Toste, R. G. Bergman, K. N. Raymond, *Chem. Rev.* **2015**, *115*, 3012–3035.
[4] D. L. Caulder, K. N. Raymond, *J. Chem. Soc. Dalton Trans.* **1999**, 1185–1200.
[5] T. Sawada, A. Matsumoto, M. Fujita, *Angew. Chem. Int. Ed.* **2014**, *53*, 7228–7232.
[6] A. M. Castilla, W. J. Ramsay, J. R. Nitschke, *Acc. Chem. Res.* **2014**, *47*, 2063–2073.
[7] C. T. McTernan, J. A. Davies, J. R. Nitschke, *Chem. Rev.* **2022**, *122*, 10393–10437.
[8] T. R. Cook, Y. R. Zheng, P. J. Stang, *Chem. Rev.* **2013**, *113*, 734–777.
[9] K. E. Jelfs, *Ann. N. Y. Acad. Sci.* **2022**, *1518*, 106–119.
[10] T. K. Piskorz, V. Martí-Centelles, T. A. Young, P. J. Lusby, F. Duarte, *ACS Catal.* **2022**, *12*, 5806–5826.
[11] B. H. Northrop, Y. R. Zheng, C. H. I. Ki-Whan, P. J. Stang, *Acc. Chem. Res.* **2009**, *42*, 1554–1563.
[12] W. M. Bloch, G. H. Clever, *Chem. Commun.* **2017**, *53*, 8506–8516.
[13] O. Jurček, P. Bonakdarzadeh, E. Kalenius, J. M. Linnanto, M. Groessl, R. Knochenmuss, J. A. Ihalainen, K. Rissanen, *Angew. Chem. Int. Ed.* **2015**, *54*, 15462–15467.
[14] K. Wu, E. Benchimol, A. Baksi, G. H. Clever, *Nat. Chem.* **2024**, *16*, 584–591.
[15] E. Benchimol, I. Regeni, B. Zhang, M. Kabiri, J. J. Holstein, G. H. Clever, *J. Am. Chem. Soc.* **2024**, *146*, 6905–6911.
[16] T. Sawada, M. Fujita, *Chem* **2020**, *6*, 1861–1876.
[17] T. Sawada, A. Saito, K. Tamiya, K. Shimokawa, Y. Hisada, M. Fujita, *Nat. Commun.* **2019**, *10*, 921.
[18] T. R. Schulte, J. J. Holstein, L. Schneider, A. Adam, G. Haberhauer, G. H. Clever, *Angew. Chem. Int. Ed.* **2020**, *59*, 22489–22493.
[19] T. R. Cook, P. J. Stang, *Chem. Rev.* **2015**, *115*, 7001–7045.
[20] D. L. Caulder, K. N. Raymond, *Acc. Chem. Res.* **1999**, *32*, 975–982.
[21] D. F. Brightwell, G. Truccolo, K. Samanta, E. J. Fenn, S. J. Holder, H. J. Shepherd, C. S. Hawes, A. Palma, *Chem. Eur. J.* **2022**, *28*, e202202368.
[22] D. F. Brightwell, G. Truccolo, K. Samanta, H. J. Shepherd, A. Palma, *ACS Macro Lett.* **2023**, *12*, 908–914.
[23] S. Kakinoki, Y. Hirano, M. Oka, *Polym. Bull.* **2005**, *53*, 109–115.
[24] P. Wilhelm, B. Lewandowski, N. Trapp, H. Wennemers, *J. Am. Chem. Soc.* **2014**, *136*, 15829–15832.
[25] P. Morales, M. A. Jiménez, *Arch. Biochem. Biophys.* **2019**, *661*, 149–167.
[26] T. Schnitzer, E. Paenurk, N. Trapp, R. Gershoni-Poranne, H. Wennemers, *J. Am. Chem. Soc.* **2021**, *143*, 644–648.
[27] U. Lewandowska, W. Zajaczkowski, S. Corra, J. Tanabe, R. Borrmann, E. M. Benetti, S. Stappert, K. Watanabe, N. A. K. Ochs, R. Schaeublin, C. Li, E. Yashima, W. Pisula, K. Müllen, H. Wennemers, *Nat. Chem.* **2017**, *9*, 1068–1072.
[28] B. M. Lewandowski, D. Schmid, R. Borrmann, D. Zetschok, M. Schnurr, H. Wennemers, *Nat. Synth.* **2023**, *2*, 331–337.
[29] B. E. Barber, E. M. G. Jamieson, L. E. M. White, C. T. McTernan, *Chem* **2024**, *10*, 2792–2806.
[30] N. V. Costantini, H. K. Ganguly, M. I. Martin, N. A. Wenzell, G. P. A. Yap, N. J. Zondlo, *Chem. Eur. J.* **2019**, *25*, 11356–11364.
[31] M. Yoshizawa, M. Nagao, K. Kumazawa, M. Fujita, *J. Organomet. Chem.* **2005**, *690*, 5383–5388.
[32] J. J. P. Stewart, *J. Mol. Model.* **2007**, *13*, 1173–1213.
[33] C. Bannwarth, S. Ehlert, S. Grimme, *J. Chem. Theory Comput.* **2019**, *15*, 1652–1671.
[34] S. Artemova, L. Jaillet, S. Redon, *J. Comput. Chem.* **2016**, *37*, 1191–1205.
[35] C. Adamo, V. Barone, *J. Chem. Phys.* **1999**, *110*, 6158–6170.
[36] M. Ernzerhof, G. E. Scuseria, *J. Chem. Phys.* **1999**, *110*, 5029–5036.
[37] S. Grimme, J. Antony, S. Ehrlich, H. Krieg, *J. Chem. Phys.* **2010**, *132*, 154104.
[38] S. Grimme, S. Ehrlich, L. Goerigk, *J. Comput. Chem.* **2011**, *32*, 1456–1465.
[39] F. Weigend, R. Ahlrichs, *Phys. Chem. Chem. Phys.* **2005**, *7*, 3297–3305.
[40] A. V. Marenich, C. J. Cramer, D. G. Truhlar, *J. Phys. Chem. B* **2009**, *113*, 6378–6396.
[41] K. O. Christe, W. W. Wilson, *J. Fluorine Chem.* **1990**, *46*, 339–342.
[42] C. A. Wamser, *J. Am. Chem. Soc.* **1948**, *70*, 1209–1215.
[43] E. T. Urbansky, *Chem. Rev.* **2002**, *102*, 2837–2854.
[44] W. F. Finney, E. Wilson, A. Callender, M. D. Morris, L. W. Beck, *Environ. Sci. Technol.* **2006**, *40*, 2572–2577.
[45] P. Mal, B. Breiner, K. Rissanen, J. R. Nitschke, *Science* **2009**, *324*, 1697–1699.
[46] D. A. Rothschild, A. Tran, M. C. Lipke, *Organometallics* **2023**, *42*, 3219–3226.
[47] R. Banerjee, D. Chakraborty, P. S. Mukherjee, *J. Am. Chem. Soc.* **2023**, *145*, 7692–7711.

Version of record online: ■■, ■■

RESEARCH ARTICLE

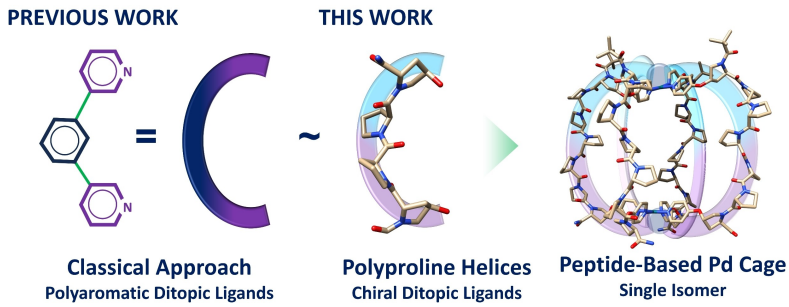

The design principles used for the synthesis of classical metallo-organic ligands have been successfully translated to polyproline peptides, a biocompatible class of chiral ligands. These peptide-based ditopic ligands have been successfully used to stereoselectively synthesize a novel Pd lantern cage, which exhibits excellent stability in water and demonstrates the stabilization of a highly reactive species in solution.

*Dr. D. F. Brightwell, Dr. K. Samanta, Dr. J. Muldoon, Dr. P. C. Fleming, Dr. Y. Ortin, Dr. L. Mardiana, Dr. P. G. Waddell, Dr. M. J. Hall, Dr. E. R. Clark, Dr. F. Fantuzzi, Dr. A. Palma**

Applying Metallo-Organic Ligand Design Principles to the Stereoselective Synthesis of a Peptide-Based $Pd_2L_4X_4$ Cage